https://doi.org/10.46813/2021-136-160

IMAGE CONVERSION OF σ- AND π-COMPONENTS OF RADIATION OF RELATIVISTIC ELECTRON AND METROLOGICAL CHARACTERISTICS OF THE PHOTON FLUX IN THE SYNCHROTRON RADIATION OUTLET

A.S. Mazmanishvili, N.V. Moskalets, A.A. Shcherbakov
National Science Center "Kharkov Institute of Physics and Technology", Kharkiv, Ukraine
E-mail: mazmanishvili@gmail.com

The paper deals with the efficiency of the capture of a photon flux of the synchrotron radiation (SR) σ- and π-components by the optical window in the SR quantum extraction channel of the NESTOR generator. It also analyses the dependence between the capture quality and different radiation wavelengths. Consideration has been given to the beam size effect on the shape and dimensions of the angular distribution of the photon flux. A model has been constructed to describe the optical imaging in the registration plane. Expressions are given for estimating the efficiency of the capture of SR quanta into the optical window of the extraction channel. The factors that exert influence on the efficiency of capturing through the window are analyzed. Examples of numerical calculations are provided for formation of the final SR spectral density of the 225 MeV relativistic electrons at the output of the optical channel. The dimensions of the optical window have been determined, which ensure the reliable registration of the total flux of SR quanta for the chosen spectral range of SR quanta wavelengths.

PACS: 29.20.-c, 41.60.Ap, 29.27.Fh

INTRODUCTION

The synchrotron radiation (SR), occurring during operation of electron storage rings, makes it possible to carry out fundamental scientific research and applied technological developments by virtue of the fact that it shows unique properties such as a continuous spectrum from infrared to X-ray regions, acute directivity, a high degree of polarization, the feasibility of exact calculation of characteristics [1, 2]. Owing to all these properties, the SR has recently begun to play a decisive role in the intensive development of the most promising research studies in physics, chemistry, biology, medicine, microelectronics, tomography, materials science, etc. [3 - 5]. The SR from bending magnets with having exactly determined parameters can act as an absolute standard in metrology [6].

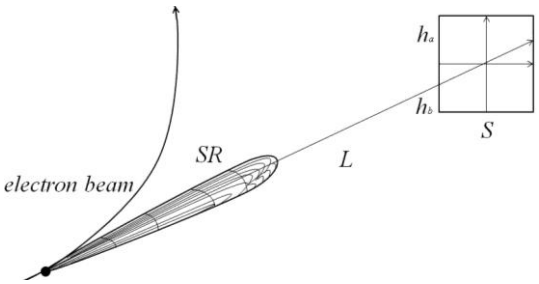

Fig. 1. Scheme for observing the flux of SR quanta

The influence of the distribution of particles oscillations across the vertical oscillations of the beam on the formation of the angular distribution of the SR was investigated in [7]. The present work deals with the efficiency of capture of the flux of σ- and π-components by the optical window in the SR quanta extraction channel (see Fig. 1). Consideration is given to the analysis of the capture quality at different radiation wavelengths. Examples of numerical calculations are presented for the formation of the final SR spectral density of a relativistic electron with the energy of 225 MeV at the output of the optical channel in the "NESTOR" generator [9 - 11].

MATHEMATICAL MODEL

The SR of a relativistic electron is characterized by a high degree of polarization. In particular, at zero angle (ψ =0) to the orbit plane, the SR is linearly polarized. The spectral-angular dependences of the flux of SR quanta are calculated in accordance with the expressions that describe the distribution density for the σ-component $w_\sigma(\psi)$ (in the orbit plane) and the π-component of the radiation $w_\pi(\psi)$ (perpendicular to the plane) [8]:

$$w_\sigma(\psi) = G\left(1+\gamma^2\psi^2\right)^2 K_{2/3}^2\left(\frac{\lambda_c}{2\lambda}\left(1+\gamma^2\psi^2\right)^{3/2}\right),$$
$$w_\pi(\psi) = G\gamma^2\psi^2\left(1+\gamma^2\psi^2\right)K_{1/3}^2\left(\frac{\lambda_c}{2\lambda}\left(1+\gamma^2\psi^2\right)^{3/2}\right), \quad (1)$$

here $G = 8\pi e_0^2 R^2 f/(3c\hbar\lambda^3\gamma^4)$, $K_{2/3}(.)$ and $K_{1/3}(.)$ are the Macdonald functions, λ is the wavelength, E is the electron energy, E_0 is the electron rest energy, $\gamma = E/E_0$ is the relativistic factor, e_0 is the electron charge, R is the radius of rotation of the magnets, f is the rotation frequency, c is the speed of light, $\hbar$ is the Planck constant, $\lambda_c = 4\pi e_0^2 Rf/(\sqrt{3}c\hbar\gamma^3)$ is the critical wavelength of radiation. The total angular density is $w(\psi)=w_\sigma(\psi)+w_\pi(\psi)$.

The photon flux of each of the electrons is characterized by an angular distribution, the axis of which coincides with the particle direction, and the top of the distribution coincides with the place of radiation site. Fig. 2 shows a family of angular flux density distributions for the σ- and π-components of polarization, calculated for one of the SR output channels in the generator. The calculation parameters in this figure and further were E=225 MeV, R=0.5 m and f=19.46 MHz, while λ_c=2.45·10^{-8} m.

The electrons in the storage ring oscillate around the equilibrium orbit. These oscillations are due to the recoil of electrons during emission of SR quanta, and also, to intrabeam scattering and scattering by residual gas particles. As a result, the beam particles are distributed around the equilibrium orbit with a normal law in 6-dimensional space.

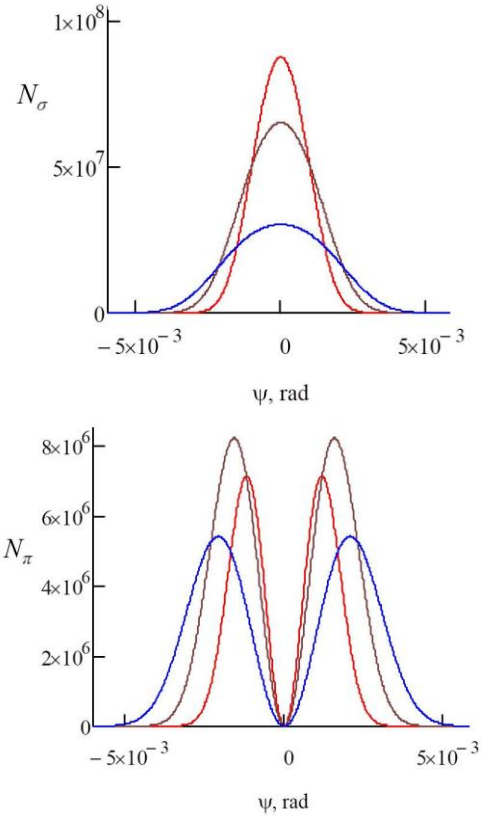

Fig. 2. Angular distributions of the flux of quanta $N_\sigma(\psi)$ and $N_\pi(\psi)$ for different wavelengths; $\lambda=0.5\lambda_c$ (red), $\lambda=\lambda_c$ (brown), $\lambda=2\lambda_c$ (blue)

Let us consider the influence of the beam particle distribution on the properties of the flux of SR quanta. The distribution in the longitudinal direction does not affect the spectral-angular characteristics of the SR quantum flux due to the azimuthal symmetry. For the same reason, the radial distribution of particles also does not affect the characteristics of the SR flux. For the vertical distribution of particles, we use the formula:

$$\rho(y,y')=\frac{1}{2\pi\sigma_y\sigma_{y'}}\exp\left(-\frac{y^2}{2\sigma_y^2}-\frac{y'^2}{2\sigma_{y'}^2}\right), \quad (2)$$

where σ_y and $\sigma_{y'}$ are the root-mean-square dimensions of the beam along y and y' respectively.

At the distance L we now consider the receiving plane perpendicular to the tangent to the radiation point on a circular orbit. We locate at the distance L an optical window of width S, with the aperture (h_a, h_b) along the vertical.

The quantum emission angle ψ, as well as the coordinates of emission (y, y') and reception h in the vertical direction are mutually related $h-\psi L=y+Ly'$. On average, the total number N_σ and N_π of photons of the σ- and π-polarization components passing through the window will be:

$$N_\sigma=\int_S ds\int_{h_b}^{h_a}dh\int_{-\pi/2}^{\pi/2}d\psi\left\langle\delta\left(h-y-y'L-\psi L\right)\right\rangle w_\sigma(\psi),$$
$$N_\pi=\int_S ds\int_{h_b}^{h_a}dh\int_{-\pi/2}^{\pi/2}d\psi\left\langle\delta\left(h-y-y'L-\psi L\right)\right\rangle w_\pi(\psi), \quad (3)$$

where $\delta(.)$ is the Dirac delta-function. In expression (3), the angle brackets denote averaging over y and y' according to (2). Taking into account the width of the receiving window leads to the multiplier:

$$\mu=\frac{S}{2\pi\sqrt{R^2+L^2}}, \quad (4)$$

so we have:

$$N_\sigma=\mu\int_{h_b}^{h_a}dh\int_{-\pi/2}^{\pi/2}d\psi\left\langle\delta\left(h-y-y'L-\psi L\right)\right\rangle w_\sigma(\psi),$$
$$N_\pi=\mu\int_{h_b}^{h_a}dh\int_{-\pi/2}^{\pi/2}d\psi\left\langle\delta\left(h-y-y'L-\psi L\right)\right\rangle w_\pi(\psi). \quad (5)$$

Bearing in mind (2), we note that at fixed ψ owing to the normality of y and y' the random variable h is also normal with the mathematical expectation ψL and the dispersion:

$$\sigma_L^2=\sigma_y^2+\sigma_{y'}^2L^2 \quad (6)$$

Therefore, for the angular distributions averaged relative to the beam, we obtain:

$$N_\sigma(h)=\frac{\mu L}{\sqrt{2\pi}\sigma_L}\int_{-\pi/2}^{\pi/2}d\psi\exp\left(-\frac{(\psi L-h)^2}{2\sigma_L^2}\right)w_\sigma(\psi),$$
$$N_\pi(h)=\frac{\mu L}{\sqrt{2\pi}\sigma_L}\int_{-\pi/2}^{\pi/2}d\psi\exp\left(-\frac{(\psi L-h)^2}{2\sigma_L^2}\right)w_\pi(\psi). \quad (7)$$

It follows from (7) that the resulting angular distribution is the convolution of the normal density associated with the beam with the angular distribution that describes the emission of quanta of the σ- and π-components of the SR. Due to the parity, the first moment of distributions (7) is equal to zero. The variance of the resulting angular distribution $\langle h^2/L^2\rangle$ will decrease with increasing L as $\sigma'^2_L=\sigma^2_{y'}+\sigma^2_y/L^2$.

By its unimodality, the distribution of quanta for the σ-component of polarization is more resistant to this effect. Considering that the angular spectrum of the π-component of polarization has two symmetric maxima, its broadening by virtue of (7) turns out to be more noticeable. In this case, with an increase in the distance L, the spatial pattern along the vertical axis will also be expanded. With decrease in the wavelength λ, the corresponding decrease in the angular dispersion of the π-component takes place $\left\langle\psi_\pi^2(\lambda)\right\rangle$, therefore, this polarization component will be normalized if $\sigma_{y'}^2>>\left\langle\psi_\pi^2(\lambda)\right\rangle$. Otherwise, the angular distribution would not be normalized for any L.

Let us perform the integration over the vertical coordinate h in formula (7) within the limits (h_a, h_b), using the integration variable $t=(h-\psi L)/\sqrt{2}\sigma_L$. Then, for

the total number of photons of the polarization components N_σ and N_π, we find:

$$N_\sigma = \frac{\mu}{2}\int_{-\pi/2}^{\pi/2} d\psi \, \mathrm{E}_1(\psi, h_a, h_b, L) w_\sigma(\psi),$$
$$N_\pi = \frac{\mu}{2}\int_{-\pi/2}^{\pi/2} d\psi \, \mathrm{E}_1(\psi, h_a, h_b, L) w_\pi(\psi), \quad (8)$$

where the function is introduced:

$$\mathrm{E}_1(\psi, h_a, h_b, L) = \mathrm{erf}\left(\frac{\psi L - h_a}{\sqrt{2}\sigma_L}\right) - \mathrm{erf}\left(\frac{\psi L - h_b}{\sqrt{2}\sigma_L}\right) \quad (9)$$

and erf(.) is the error function.

In the symmetric case, when $h_a = -h_b = H$, expressions (8) are simplified to:

$$N_\sigma = \mu\int_{-\pi/2}^{\pi/2} d\psi \, \mathrm{erf}\left(\frac{\psi L - H}{\sqrt{2}\sigma_L}\right) w_\sigma(\psi),$$
$$N_\pi = \mu\int_{-\pi/2}^{\pi/2} d\psi \, \mathrm{erf}\left(\frac{\psi L - H}{\sqrt{2}\sigma_L}\right) w_\pi(\psi). \quad (10)$$

On account of a rather small value of the variance σ_L^2, expressions (8)-(10), are difficult to use in numerical calculations. Therefore, we reduce expressions (8) to a more convenient and visual form. We use the integral functions of the angular distribution of the components. Fig. 3 shows the family of integral angular distributions of flux density σ- and π-components of polarization calculated for one of the SR output channels in the generator.

$$W_\sigma(\psi) = \int_{-\pi/2}^{\psi} d\psi' \, w_\sigma(\psi'),$$
$$W_\pi(\psi) = \int_{-\pi/2}^{\psi} d\psi' \, w_\pi(\psi'). \quad (11)$$

The calculation parameters in Fig. 3 and further were σ_y= 0.2 mm and $\sigma_{y'}$= 0.15 mrad.

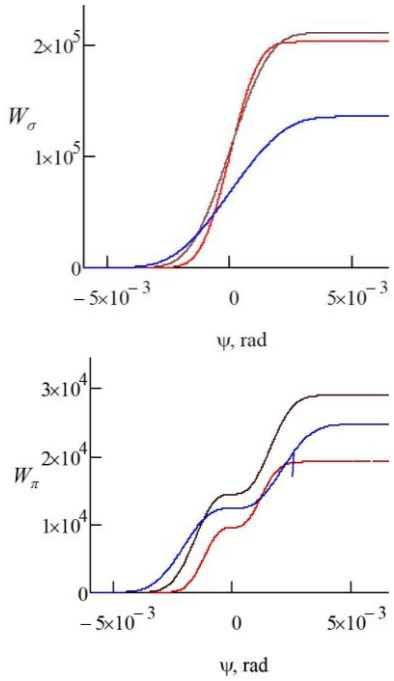

Fig. 3. Integral angular distributions of the flux of quanta $W_\sigma(\psi)$ and $W_\pi(\psi)$; $\lambda=0.5\lambda_c$ (red), $\lambda=\lambda_c$ (brown), $\lambda=2\lambda_c$ (blue)

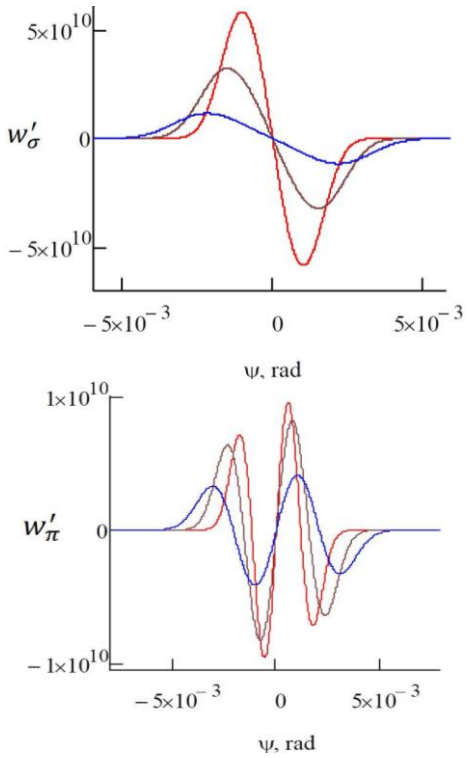

Fig. 4. Derivatives of distributions $w'_\sigma(\psi)$ and $w'_\pi(\psi)$; $\lambda=0.5\lambda_c$ (red), $\lambda=\lambda_c$ (brown), $\lambda=2\lambda_c$ (blue)

Using functions (11), we take the integrals in (8) by parts. As a result, we get:

$$N_\sigma = \frac{\mu}{2}\int_{-\pi/2}^{\pi/2} d\psi \, \mathrm{E}_2(\psi, h_a, h_b, L) W_\sigma(\psi),$$
$$N_\pi = \frac{\mu}{2}\int_{-\pi/2}^{\pi/2} d\psi \, \mathrm{E}_2(\psi, h_a, h_b, L) W_\pi(\psi), \quad (12)$$

where the following function is introduced:

$$\mathrm{E}_2(\psi, h_a, h_b, L) = \frac{1}{\sqrt{2\pi}\sigma_L} \times \left[\exp\left(-\frac{(\psi L - h_a)^2}{2\sigma_L^2}\right) - \exp\left(-\frac{(\psi L - h_b)^2}{2\sigma_L^2}\right)\right]. \quad (13)$$

Due to the smallness of σ_L the exponents in (13) have the filtering property. Therefore, only the regions around the points $\psi_a = h_a/L$ and $\psi_b = h_b/L$ of size $(-3\sigma_L; 3\sigma_L)$ each, will contribute to integrals (12). Thus they take the forms:

$$N_\sigma = \frac{\mu}{\sqrt{2\pi}\sigma_L} \times \int_{-3\sigma_L}^{3\sigma_L} d\xi \exp\left(-\frac{\xi^2}{2\sigma_L^2}\right)\left[W_\sigma\left(\frac{h_a + \xi}{L}\right) - W_\sigma\left(\frac{h_b + \xi}{L}\right)\right],$$
$$N_\pi = \frac{\mu}{\sqrt{2\pi}\sigma_L} \times \int_{-3\sigma_L}^{3\sigma_L} d\xi \exp\left(-\frac{\xi^2}{2\sigma_L^2}\right)\left[W_\pi\left(\frac{h_a + \xi}{L}\right) - W_\pi\left(\frac{h_b + \xi}{L}\right)\right]. \quad (14)$$

It follows from (14) that for $\sigma_L \to 0$ the leading terms are equal to:

ISSN 1562-6016. ВАНТ. 2021. №6(136)

$$N_\sigma = \mu[W_\sigma(\psi_a) - W_\sigma(\psi_b)]\,,$$
$$N_\pi = \mu[W_\pi(\psi_a) - W_\pi(\psi_b)] \qquad (15)$$

and correspond to the boundary angles ψ_a and ψ_b of quantum flux capture by the window. Due to the ψ parity with respect to the angular functions $w_\sigma(\psi)$ and $w_\pi(\psi)$ the terms linear in σ_L vanish.

The corrections quadratic in σ_L are:

$$\Delta^{(2)}N_\sigma = \mu\frac{\sigma_L^2}{2L^2}[w'_\sigma(\psi_a) - w'_\sigma(\psi_b)],$$
$$\Delta^{(2)}N_\pi = \mu\frac{\sigma_L^2}{2L^2}[w'_\pi(\psi_a) - w'_\pi(\psi_b)], \qquad (16)$$

where $w'_\sigma(\psi)$ and $w'_\pi(\psi)$ are the derivatives of the angular functions $w_\sigma(\psi)$ and $w_\pi(\psi)$ (Fig. 4).

In the symmetric case, when $h_a = -h_b = H$, expressions (10)-(12) admit the representation:

$$N_\sigma = \mu\left(W_\sigma(\psi_a) - W_\sigma(-\psi_a) + \frac{\sigma_L^2}{L^2}w'_\sigma(\psi_b)\right),$$
$$N_\pi = \mu\left(W_\pi(\psi_a) - W_\pi(-\psi_a) + \frac{\sigma_L^2}{L^2}w'_\pi(\psi_b)\right). \qquad (17)$$

NUMERICAL RESULTS

We now present the numerical calculation data on the spectral-angular flux of the number of emitted SR quanta. The calculations were carried out for the case of the window of width S=0.06 m and vertical dimensions H=0.05 m. Thus, at the base distance L=3 m, the capture angle was ψ_a=10 mrad.

The calculations were carried out under the assumption that a single electron revolves in the orbit.

Fig. 5 shows the number of captured quanta N_σ versus the emission wavelength λ for different capture angles. For comparison, the functions N_σ are shown for H=0.05 m, H=0.02 m and H=0.01 m. It can be seen that starting from the wavelength λ=1·10^{-7} m, the number of photons decreases, falling at λ=1·10^{-5} m by a factor of ~100.

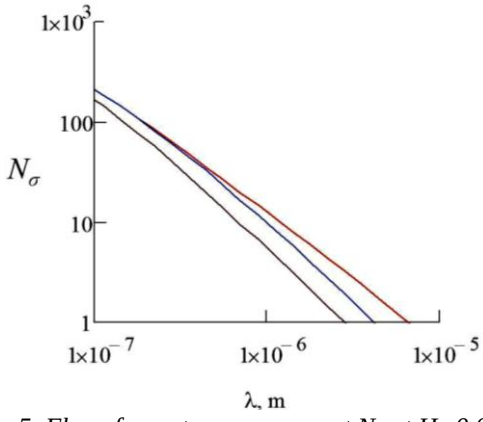

Fig. 5. Flux of quanta σ-component N_σ at H=0.05 m (red), H=0.02 m (brown), H=0.01 m (blue)

Similar dependences for the number N_π captured quanta on the wavelength λ are shown in Fig. 6.

In the π-component case, the decrease is more noticeable; moreover, it begins at shorter wavelengths λ=10$^{-8.5}$ m. This is due to the fact that the peripheral parts of the angular distribution $w_\sigma(\psi)$ are more pronounced than those of the distribution $w_\pi(\psi)$.

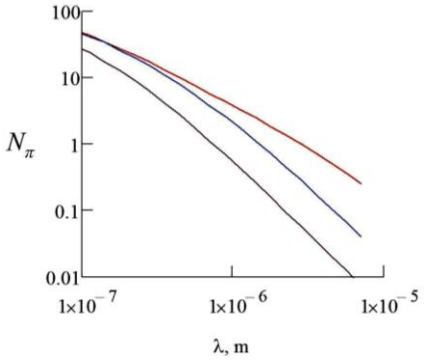

Fig. 6. Flux of quanta of π-component N_π at H=0.05 m (red), H=0.02 m (blue), H=0.01 m (brown)

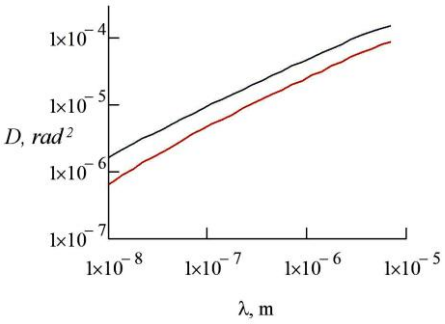

Fig. 7. Dispersions D of angular distributions of the σ-component $D_\sigma(\lambda)$ (red) and π-component $D_\pi(\lambda)$ (blue)

From Fig. 2 it can be seen that the density of the π-component occupies a larger angular interval than the density of the σ-component. The calculated dependences for the variances of the angular distributions $D_\sigma(\lambda) = \langle\psi_\sigma^2(\lambda)\rangle$ and $D_\pi(\lambda) = \langle\psi_\pi^2(\lambda)\rangle$ are shown in Fig. 7.

From Fig. 7 it is evident that the angular dispersion of the π-component is nearly twofold greater than that of the σ-component. This property leads to a less efficient capture of π-component photons into the window.

CONCLUSIONS

From the given dependences it follows that the main factors determining the capture of the quantum flux in the channel are the vertical size H of the window and the standard deviations of the angular distributions $S_\sigma(\lambda) = D_\sigma^{1/2}(\lambda)$ and $S_\pi(\lambda) = D_\pi^{1/2}(\lambda)$. With an increase in the wavelength λ, the $LS_\sigma(\lambda)$ and $LS_\pi(\lambda)$ approach the value of H values approach the H value, and hence, the capture efficiency is also influenced by the peripheral parts of the distributions $w_\sigma(\psi)$ and $w_\pi(\psi)$.

Fig. 8 shows the wavelength λ dependences of the fraction $\varepsilon(\lambda)$ of quanta that are not captured in the window It can be seen that at $\lambda \le 5\cdot10^{-7}$ m the capture into the window with having the angular opening (-3; +3) mrad occurs with a sufficiently high efficiency. With a further increase in the wavelength, the fraction of uncaptured quanta increases. Moreover, this value is larger for the π-component, quanta. The reason is that the standard deviation of the π-component $S_\pi(\lambda)$ always exceeds the standard deviation $S_\sigma(\lambda)$ of the σ-component of the SR.

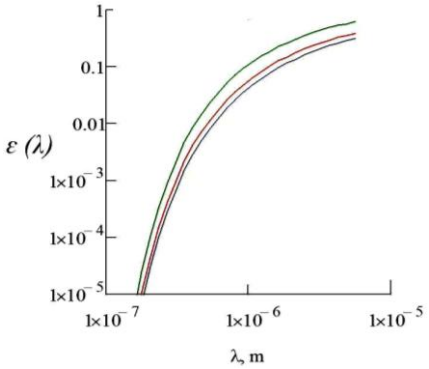

Fig. 8. Fractions $\varepsilon(\lambda)$ of uncaptured quanta N_σ (blue), N_π (green) and total flux of quanta $N_\sigma+N_\pi$ (red)

In channels with an increased base length L, it is the standard deviation of the angular distributions $S_\sigma(\lambda)$ and $S_\pi(\lambda)$ that will exert a decisive influence on the formation of angular distributions in the receiving plane and, accordingly, on the efficiency of the capture of photon fluxes.

REFERENCES

1. E.E. Koch, D.E. Eastman, Y. Farge. *Handbook on synchrotron radiation* / Ed. E.-E. Koch. 1983, v. 1a, Amsterdam, p. 1-64.
2. I.M. Ternov, V.V. Mikhailin. *Synchrotron radiation. Theory and experiment*. M.: "Energoatomizdat", 1986, p. 219-250.
3. A.M. Pravilov. *Radiometry in Modern Scientific Experiments.* "SpringerWienNewYork", 2011.
4. V.E. Ivashenko, I.M. Karnaukhov, et al. Utilization of synchrotron radiation of the N-100 M storage ring for research in solid state physics // *Problems of Atomic Science and Technology. Series "Nuclear Physics Investigations"*. 2004, № 6, p. 164-166. http://dspace.nbuv.gov.ua/handle/123456789/81344.
5. J.B. Pelka. Synchrotron radiation in biology and medicine // *Acta Physica Polonica (114).* 2008, № 2, p. 309-329. http://przyrbwn.icm.edu.pl/APP/PDF/114/a114z202.pdf.
6. Roman Klein, Guido Brandt, et al. Operation of the Metrology Light Source as a primary radiation source standard // *Phys. Rev. ST Accel. Beams 11*. 2008.
7. A.S. Mazmanishvili, N.V. Moskalets. Formation of optical images with synchrotron radiation flux of relativistic electrons in the X-ray generator "NESTOR" // *East. Eur. J. Phys. **3**, XX. 2021*. https://doi.org/10.26565/2312-4334-2021-3-01.
8. G. Bruk. *Cyclic charged particle accelerators*. Moscow: "Atomizdat", 1970.
9. I.M. Karnaukhov et al. Synchrotron radiation from the NESTOR storage ring // *Problems of Atomic Science and Technology. Series "Nuclear Physics Investigations"*. 2007, № 5, p. 156-159. https://vant.kipt.kharkov.ua/TABFRAME.html.
10. A.A. Shcherbakov et al. The Kharkov X-ray generator facility NESTOR// *4th International Particle Accelerator Conference*, (IPAC, Shanghai, 2013), p. 2253-2255. http://hal.in2p3.fr/in2p3-00823292.
11. V. Androsov et al. Commissioning of the storage ring for the Kharkov generator of X-ray radiation NESTOR // *9th International Particle Accelerator Conference*. IPAC, Vancouver, 2018, p. 4307-4309. https://accelconf.web.cern.ch/ipac2018/papers/thpmk008.pdf.

Article received 27.09.2021

ПРЕОБРАЗОВАНИЕ ИЗОБРАЖЕНИЙ σ- И π-КОМПОНЕНТ ИЗЛУЧЕНИЯ РЕЛЯТИВИСТСКИХ ЭЛЕКТРОНОВ И МЕТРОЛОГИЧЕСКИЕ ХАРАКТЕРИСТИКИ ПОТОКА ФОТОНОВ В КАНАЛЕ ВЫВОДА СИНХРОТРОННОГО ИЗЛУЧЕНИЯ

А.С. Мазманишвили, Н.В. Москалец, А.А. Щербаков

Изучена эффективность захвата потока фотонов σ- и π-компонент синхротронного излучения (СИ) оптическим окном в канале вывода квантов СИ, и проанализирована зависимость качества захвата для различных длин волн излучения. Проведен учет размеров пучка на форму и размеры углового распределения потока фотонов. Построена модель, описывающая формирование оптического изображения в плоскости регистрации. Предложены выражения, позволяющие оценить эффективность захвата квантов СИ в оптическое окно канала вывода. Проанализированы факторы, влияющие на эффективность захвата в окно. Представлены примеры численного расчета по формированию итоговой спектральной плотности СИ релятивистского электрона с энергией 225 МэВ на выходе оптического канала. Получены размеры оптического люка, величина которых позволяет гарантированно регистрировать весь поток квантов СИ для выбранного спектрального диапазона волн квантов СИ.

ПЕРЕТВОРЕННЯ ЗОБРАЖЕНЬ σ- І π-КОМПОНЕНТ ВИПРОМІНЮВАННЯ РЕЛЯТИВІСТСЬКИХ ЕЛЕКТРОНІВ І МЕТРОЛОГІЧНІ ХАРАКТЕРИСТИКИ ПОТОКУ ФОТОНІВ У КАНАЛІ ВИВЕДЕННЯ СИНХРОТРОННОГО ВИПРОМІНЮВАННЯ

О.С. Мазманішвілі, Н.В. Москалець, О.О. Щербаков

Вивчена ефективність захоплення потоку фотонів σ- і π-компонент синхротронного випромінювання (СВ) оптичним вікном у каналі виведення квантів СВ, і проаналізована залежність якості захоплення для різних довжин хвиль випромінювання. Проведено облік розмірів пучка на форму і розміри кутового розподілу потоку фотонів. Побудована модель, що описує формування оптичного зображення в площині реєстрації. Запропоновано вирази, що дозволяють оцінити ефективність захоплення квантів СВ у оптичне вікно каналу виведення. Проаналізовано фактори, що впливають на ефективність захоплення у вікно. Представлені приклади чисельного розрахунку з формування підсумкової спектральної щільності СВ релятивістського електрона з енергією 225 МеВ на виході оптичного каналу. Отримано розміри оптичного люка, величина яких дозволяє гарантовано реєструвати весь потік квантів СВ для обраного спектрального діапазону хвиль квантів СВ.